中国激光

2.794 μm高重复频率Fe^{2+}:ZnSe被动调Q激光器脉冲特性理论分析与实验研究

熊正东[1,2]，姜玲玲[1,2]，程庭清[1]，江海河[1,2*]

[1]中国科学院合肥物质科学研究院健康与医学技术研究所，安徽 合肥 230031；

[2]中国科学技术大学，安徽 合肥 230031

摘要 3 μm波段被动调Q激光可饱和吸收体的损伤阈值较低，在高峰值功率、高重复频率条件下非常容易出现损伤。理论分析了可饱和吸收体的初始透过率和输出镜的反射率对被动调Q激光输出脉冲宽度的影响。采用两种具有不同初始透过率的Fe^{2+}:ZnSe晶体进行了氙灯泵浦的Er,Cr:YSGG激光器被动调Q实验研究。结果表明，具有低初始透过率的可饱和吸收体能够获得较低的脉冲宽度，且具有高初始透过率的可饱和吸收体能够通过提高输出镜的反射率来压缩脉冲宽度，脉冲宽度与晶体棒直径无关，实验结果与理论结果吻合。通过优化腔内布局实现了高重复频率、高峰值功率的2.794 μm被动调Q激光输出，激光器在60 Hz重复频率下分别获得了单脉冲能量4.7 mJ和7.0 mJ的调Q激光输出，脉冲宽度分别为97.0 ns和72.6 ns。研究结果为被动调Q激光器的设计提供了理论指导。

关键词 激光器；固体激光器；Er, Cr:YSGG激光；被动调Q；Fe^{2+}:ZnSe

中图分类号 TN248.1 **文献标志码** A **DOI**: 10.3788/CJL220800

1 引 言

3 μm波段对应水的吸收峰位置，3 μm波段激光在生物医学、非线性光学、危险化学品检测、大气遥感和污染监测等领域中有着广泛的应用[1-5]。在中红外参量泵浦源中或消融牙齿硬组织时，需要较高的重复频率和较短的纳秒级脉冲宽度以提高参量光光转换率和降低消融过程中的热效应。调Q技术是获得高峰值功率、窄脉冲宽度激光的主要方式。目前，电光调Q激光技术在3 μm波段已经获得了高峰值功率的激光输出。但是，由于偏振光热退偏效应的影响，电光调Q激光的重复频率无法提高[6]；声光调Q激光技术能够实现高重复频率运转，但由于受制于声光晶体的衍射效率，无法实现大能量输出；机械调Q由于高速运动而难以精确控制，不易获得稳定的激光输出；理论上，被动调Q激光只要激光元器件的损伤阈值足够大，就能够实现高重复频率、高峰值功率的纳秒激光输出，而且被动调Q激光具有腔型结构紧凑等优点，有利于应用。

目前，许多材料已被证实适用于3 μm波段激光可饱和吸收体，如MoS_2[7]、黑磷[8-9]、石墨烯[10]、InAs[11]、乙醇[12]、Fe^{2+}:ZnSe[13-15]等。其中，只有Fe^{2+}:ZnSe晶体等少数性能相对稳定的材料能够实现较大能量的被动调Q激光输出。该晶体在短脉冲情况下的损伤阈值仅为1.5～2.0 J/cm^2@100 ns[15]，在高峰值功率、高重复频率下进行被动调Q实验时容易出现激光损伤，已报道的晶体毫焦级能量调Q激光输出都在10 Hz以内运转。因此，有必要对该晶体的被动调Q激光脉冲的输出特性进行理论分析，以减小被动调Q激光运转过程中可饱和吸收体损伤的可能性。

本文主要理论计算了Fe^{2+}:ZnSe晶体作为可饱和吸收体时的初始透过率和输出镜反射率对调Q激光输出脉冲宽度的影响。在含有不同尺寸晶体棒的激光系统中实现了闪光灯泵浦Er,Cr:YSGG被动调Q激光运转，得到的脉冲宽度与理论值基本一致。设计了重复频率为60 Hz的Er,Cr:YSGG被动调Q脉冲激光系统，其实现了高峰值功率、高重复频率的运行。

2 理论分析

Er,Cr:YSGG晶体2.79 μm激光上能级$^4I_{11/2}$的寿命长达1.4 ms，便于激活离子Er^{3+}的储能，有利于调Q激光系统输出巨脉冲激光。掺入敏化离子Cr^{3+}后，系

收稿日期：2022-04-28；**修回日期**：2022-05-13；**录用日期**：2022-05-17；**网络首发日期**：2022-05-27

基金项目：国家重点研发计划(2018YFB0407204)

通信作者：*hjiang@aiofm.ac.cn

统可有效地从泵浦氙灯光源中吸收较多的能量，并将其转移给激活离子，从而氙灯的泵浦效率得到提高。激活离子 Er^{3+} 为准三能级系统，其被动调 Q 激光的输出脉冲宽度可通过速率方程进行推导。理论上，调 Q 激光系统的输出能量(E_p)和峰值功率[16](p)可表示为

$$E_p=\frac{hvV}{2\gamma\sigma}\ln(1/R)\ln\left(\frac{n_i}{n_f}\right),\tag{1}$$

$$p=\frac{hvVl_0}{2c\gamma}\ln(1/R)\left[n_i-n_{th}-n_{th}\ln\left(\frac{n_i}{n_{th}}\right)\right],\tag{2}$$

式中：h 为普朗克常数；v 为激光频率；V 为激光介质内的模体积大小；受激辐射截面 $\sigma=5.2\times10^{-25}\ m^2$；$\gamma$ 为反转衰减因子；l_0 为谐振腔的光学长度；c 为光在真空中的速度；R 为输出镜的反射率；n_i、n_{th}、n_f 分别为初始、阈值、剩余反转粒子数密度，它们可由被动调 Q 的速率方程求得[17]：

$$n_{th}=\frac{\ln\frac{1}{R}+L}{2\sigma l},\tag{3}$$

$$n_i=\frac{\ln\frac{1}{T_0^2}+\ln\frac{1}{R}+L}{2\sigma l},\tag{4}$$

$$n_i-n_f-n_{th}\ln\frac{n_i}{n_f}=0,\tag{5}$$

式中：T_0 为可饱和吸收体的初始透过率；L 为谐振损耗系数，取 0.02；l 为激光介质 Er,Cr:YSGG 晶体的长度。那么被动调 Q 激光的输出脉冲宽度 t 可表示为输出能量和峰值功率的比值：

$$t=\frac{E_p}{p}=\frac{\frac{l_0}{c}\ln\left(\frac{n_i}{n_f}\right)}{\sigma\left[n_i-n_{th}-n_{th}\ln\left(\frac{n_i}{n_{th}}\right)\right]}。\tag{6}$$

从式(6)可以看出，在激光介质选定的情况下，被动调 Q 激光的输出脉冲宽度主要由可饱和吸收体的初始透过率 T_0 和输出镜的反射率 R 所决定。

我们理论计算了在输出镜反射率分别为 30%、40%、50%、60%、70% 时输出脉冲宽度随可饱和吸收体初始透过率的变化，如图 1 所示。可以看出，被动调 Q 激光的输出脉冲宽度随着初始透过率的增加而逐渐变宽。在初始透过率一定时，输出脉冲宽度与输出镜反射率相关。当可饱和吸收体的初始透过率较低时，反射率越小，输出脉冲宽度越窄；而当初始透过率较高时，反射率越高就越容易得到较窄的脉冲宽度。

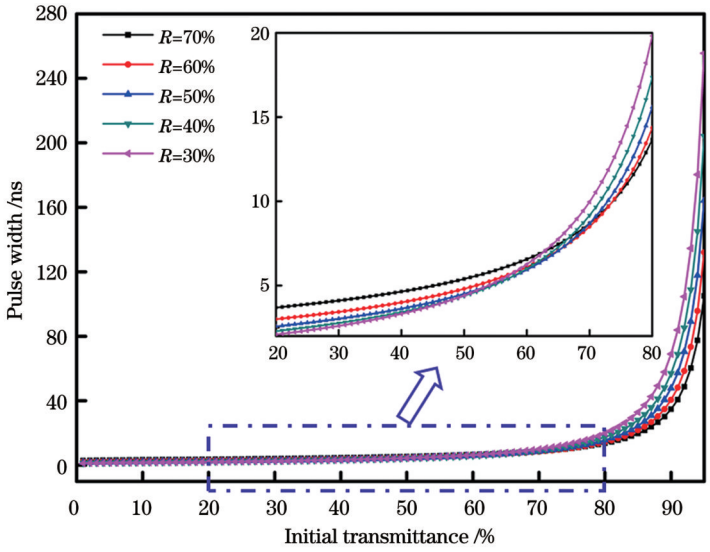

图 1　输出脉冲宽度随可饱和吸收体初始透过率的变化

Fig. 1　Output pulse width versus initial transmittance of saturable absorber

3　实验装置

本实验装置如图 2 所示，Er,Cr:YSGG 晶体棒的尺寸为 Φ3 mm× 100 mm 和 Φ4 mm×100 mm，Cr^{3+} 的原子数分数为 3%，Er^{3+} 的原子数分数为 30%，晶体棒两端镀有 2.79 μm 增透膜。谐振腔为平平腔型结构，几何腔长为 185 mm。M_1 为全反镜，在 2.79 μm 波长下反射率>99%。鉴于当前可饱和吸收体损伤阈值较低的实际情况，低输出镜反射率和高可饱和吸收体初始透过率能够减小损伤的风险。耦合输出镜 M_2 在 2.79 μm 处的内腔面反射率分别为 30% 和 40%，另一面镀有 2.79 μm 增透膜。被动调 Q 器件采用两块 Fe^{2+}:ZnSe 晶体，Fe^{2+} 浓度分别为 $5\times10^{17}/cm^3$ 和 $1.0\times10^{18}/cm^3$，尺寸分别为 7.0 mm×7.0 mm×1.5 mm 和 10.0 mm×10.0 mm×1.0 mm。双面镀有 2.79 μm 增透膜，实验过程中采用热沉通水冷却，在 2.79 μm 波段的理论透过率为 93.6% 和 91.9%。

实验采用氙灯泵浦，放电脉冲宽度为 200 μs，为保证激光器安全稳定工作，我们用去离子水对其进行冷却，水温为(293.0±0.1)K，流量为 33 L/min，大流量

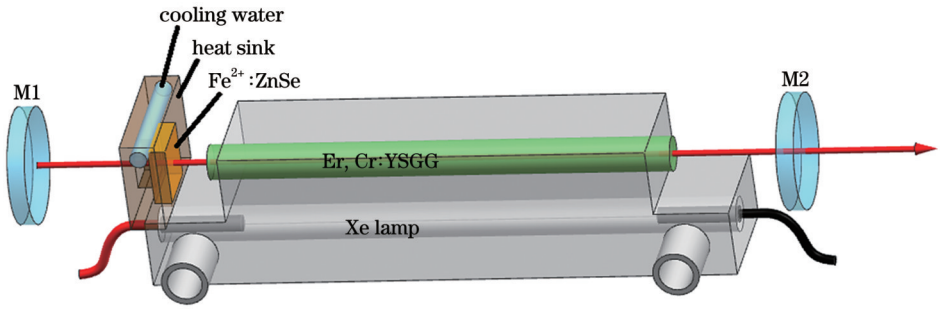

图 2　实验装置示意图

Fig. 2　Schematic of experimental device

可保证高的冷却效率。

4　结果与分析

表 1 展示了 10 Hz 下平平腔型激光系统的被动调 Q 脉冲激光的实验结果，该系统由两种具有不同初始透过率的 Fe^{2+}:ZnSe 晶体及两种尺寸的 Er,Cr:YSGG 晶体组成。调 Q 激光的脉冲宽度利用光电探测器测量获得，激光脉冲能量利用能量计测量。谐振腔内可饱和吸收体端面附近的光斑直径采用刀口法测量。

表 1　被动调 Q 激光的理论与实验结果

Table 1　Theoretical and experimental results of passive Q-switched laser

Initial transmittance of saturable absorber	Method	Size of laser crystal rod	Result	
			R=40%	R=30%
93.6%	Numerical		Pulse width of 134.1 ns	Pulse width of 167.1 ns
	Experimental	Φ3 mm×100 mm	Pulse width of 140.6 ns, pulse energy of 4.2 mJ, spot diameter of 1.36 mm	Pulse width of 161.0 ns, pulse energy of 3.9 mJ, spot diameter of 1.30 mm
		Φ4 mm×100 mm	Pulse width of 146.7 ns, pulse energy of 6.1 mJ, spot diameter of 1.64 mm	Pulse width of 175.0 ns, pulse energy of 6 mJ, spot diameter of 1.68 mm
91.9%	Numerical		Pulse width of 82.0 ns	Pulse width of 100.9 ns
	Experimental	Φ3 mm×100 mm	Pulse width of 81.0 ns, pulse energy of 6.3 mJ, spot diameter of 1.33 mm	Pulse width of 91.8 ns, pulse energy of 6.1 mJ, spot diameter of 1.31 mm
		Φ4 mm×100 mm	Pulse width of 83.3 ns, pulse energy of 8.7 mJ, spot diameter of 1.60 mm	Pulse width of 89.2 ns, pulse energy of 8.9 mJ, spot diameter of 1.67 mm

图 3 为 10 Hz 下实验中测得的激光被动调 Q 脉冲波形。从图 3 和表 1 可以看出，在可饱和吸收体初始透过率较高时，具有不同初始透过率的可饱和吸收体输出激光的脉冲宽度都是随着输出镜反射率的增加而变窄，可饱和吸收体的初始透过率越低，越容易获得大能量、窄脉宽的调 Q 激光输出。该实验结果验证了我们之前理论分析和计算的正确性。同时，激光输出脉冲宽度与晶体棒尺寸关系不大，两种晶体棒尺寸下实验测得的脉冲宽度相近。从谐振腔内的光斑直径可以看出，直径较大的晶体棒改变了谐振腔内的模体积，明显增大了输出激光能量，但腔内的激光能量密度并没有因为光斑的增大而变大，从而没有影响可饱和吸收体的漂白过程。

为了实现高重复频率运行，基于以上分析，我们研制了高重复频率的 Fe^{2+}:ZnSe 晶体被动调 Q 激光系统，该系统采用 Φ3 mm×100 mm 尺寸的 Er,Cr:YSGG 晶体，设计了凹凸腔型谐振腔结构，凹面镜 M_3 为全反镜（曲率半径 R_1=200 mm），平凸透镜 M_4 为输出镜，其凸面（曲率半径 R_2=−216 mm）在 2.79 μm 处的反射率为 70%，平面镀有 2.79 μm 增透膜。60 Hz 工作频率下的被动调 Q 激光实验表明，该腔型能够有效地补偿激光器在高重复频率下的热透镜焦距，扩大谐振腔内的光斑。通过优化 60 Hz Er,Cr:YSGG 被动调 Q 激光系统的腔内元件布局，实现了 2.794 μm 波长被动调 Q 激光输出（图 4），两种 Fe^{2+}:ZnSe 晶体的激光脉冲波形如图 5 所示。

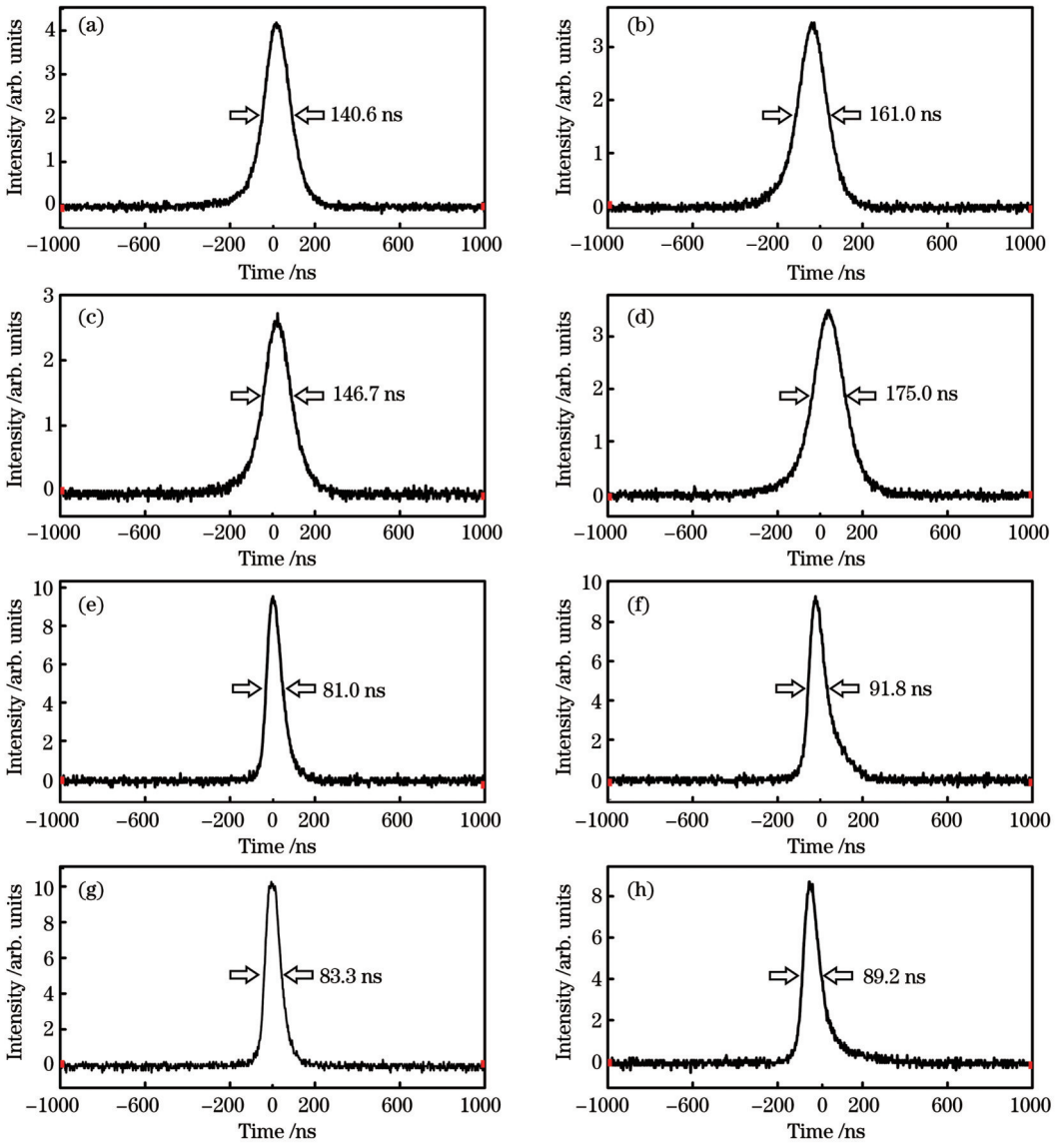

图 3　不同参数下激光调 Q 实验中测得的输出脉冲波形图。(a) T_0=93.6%, R=40%, Φ3 mm×100 mm; (b) T_0=93.6%, R=30%, Φ3 mm×100 mm; (c) T_0=93.6%, R=40%, Φ4 mm×100 mm; (d) T_0=93.6%, R=30%, Φ4 mm×100 mm; (e) T_0=91.9%, R=40%, Φ3 mm×100 mm; (f) T_0=91.9%, R=30%, Φ3 mm×100 mm; (g) T_0=91.9%, R=40%, Φ4 mm×100 mm; (h) T_0=91.9%, R=30%, Φ4 mm×100 mm

Fig. 3　Output pulse waveforms measured in laser Q-switching experiments under different parameters. (a) T_0=93.6%, R=40%, Φ3 mm×100 mm; (b) T_0=93.6%, R=30%, Φ3 mm×100 mm; (c) T_0=93.6%, R=40%, Φ4 mm×100 mm; (d) T_0=93.6%, R=30%, Φ4 mm×100 mm; (e) T_0=91.9%, R=40%, Φ3 mm×100 mm; (f) T_0=91.9%, R=30%, Φ3 mm×100 mm; (g) T_0=91.9%, R=40%, Φ4 mm×100 mm; (h) T_0=91.9%, R=30%, Φ4 mm×100 mm

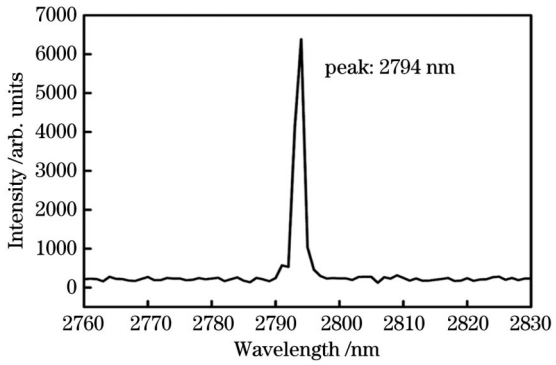

图 4　Φ3 mm×100 mm Er,Cr:YSGG 晶体 60 Hz 激光调 Q 实验中测得的输出光谱图

Fig. 4　Output spectrum measured in laser Q-switching experiment with Φ3 mm×100 mm Er, Cr : YSGG crystal at 60 Hz

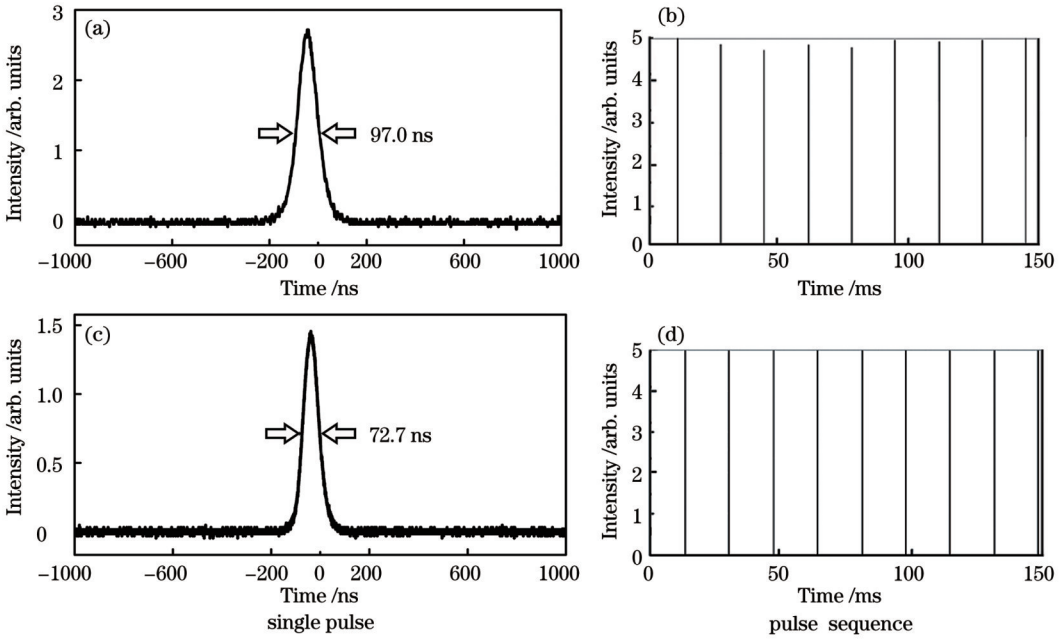

图 5　Φ3 mm×100 mm Er,Cr:YSGG 晶体 60 Hz 激光调 Q 实验中测得的输出脉冲波形图。(a)(b)T_0=93.6%;(c)(d)T_0=91.9%

Fig. 5　Output pulse waveforms measured in laser Q-switching experiment with Φ3 mm×100 mm Er, Cr : YSGG crystal at 60 Hz. (a)(b) T_0=93.6%; (c)(d) T_0=91.9%

初始透过率为 93.6% 的可饱和吸收体通过被动调 Q 获得了单脉冲宽度为 97.0 ns、脉冲能量为 4.7 mJ 的激光输出[图 5(a)],水平方向的光束质量因子为 M_x^2=8.17,M_y^2=7.84[图 6(a)];初始透过率为 91.9% 的可饱和吸收体通过被动调 Q 获得了单脉冲宽度为 72.7 ns、脉冲能量为 7.0 mJ 的激光输出[图 5(c)],水平方向的光束质量因子为 M_x^2=8.49,M_y^2=8.35[图 6(b)]。该实验进一步压缩了调 Q 激光的脉冲宽度、提高了激光脉冲的峰值功率,也证明了高的输出镜反射率能够增大腔内功率密度并有效地压缩脉冲宽度。

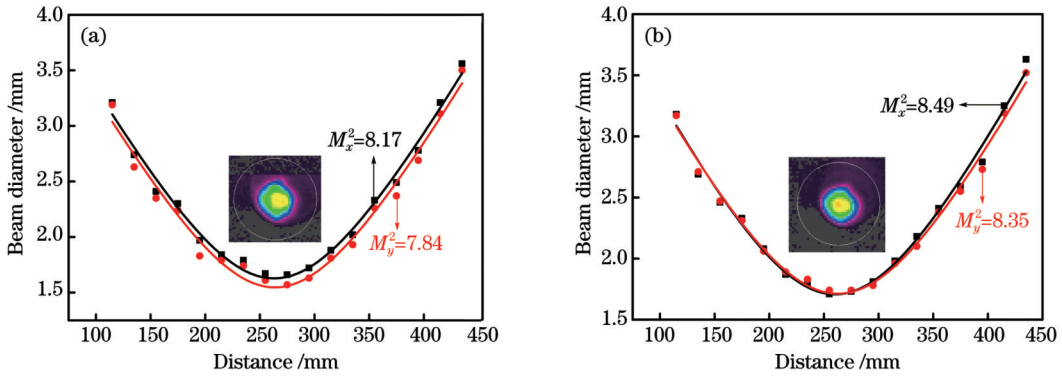

图 6　不同 T_0 下测得的光束质量因子。(a)T_0=93.6%;(b)T_0=91.9%

Fig. 6　Measured beam quality factors under different T_0. (a) T_0=93.6%; (b) T_0=91.9%

5　结　　论

理论计算了可饱和吸收体 Fe^{2+}:ZnSe 晶体在不同初始透过率下的输出脉冲宽度,分别探究了晶体棒的直径和输出镜反射率对被动调 Q 激光器的输出脉冲宽度的影响。理论与实验结果表明,晶体棒的直径对输出脉冲宽度没有影响,大的晶体棒直径有利于获得高的输出能量。提高输出镜的反射率以及降低可饱和吸收体的初始透过率都能够有效地压缩输出激光脉冲宽度,这对于被动调 Q 激光器的设计具有一定指导意义。在此理论基础上设计了氙灯泵浦 Er,Cr:YSGG 激光器,实现了 60 Hz 的高重复频率、高峰值功率的被动调 Q 激光脉冲的运行输出。

参　考　文　献

[1] 江健涛, 魏蒙恩, 熊正东, 等. 子脉冲序列模式 Er:YAG 激光消融牙本质的实验观察[J]. 中国激光, 2021, 48(1): 0107001.
Jiang J T, Wei M E, Xiong Z D, et al. Observation of dentin ablation using an Er: YAG laser in a sub-pulse sequence mode[J]. Chinese Journal of Lasers, 2021, 48(1): 0107001.

[2] 权聪, 孙敦陆, 罗建乔, 等. 氙灯抽运 Er:YAP 晶体的中红外激光性能[J]. 中国激光, 2019, 46(4): 0401003.
Quan C, Sun D L, Luo J Q, et al. Mid-infrared laser performances of Er: YAP crystals pumped by xenon lamp[J]. Chinese Journal of Lasers, 2019, 46(4): 0401003.

[3] Sanamyan T, Kanskar M, Xiao Y, et al. High power diode-pumped 2.7-μm Er^{3+}∶Y_2O_3 laser with nearly quantum defect-limited efficiency [J]. Optics Express, 2011, 19(S5): A1082-A1087.
[4] Tokita S, Murakami M, Shimizu S, et al. 12 W *Q*-switched Er∶ZBLAN fiber laser at 2.8 μm[J]. Optics Letters, 2011, 36(15): 2812-2814.
[5] 杨经纬, 江海河, 王礼, 等. 调*Q*和静态Er∶YAG激光消融骨硬组织的研究[J]. 中国激光, 2013, 40(s1): s104001.
Yang J W, Jiang H H, Wang L, et al. Study on ablation hard tissue using *Q*-switched Er∶YAG laser and free-running Er∶YAG lasers[J]. Chinese Journal of Lasers, 2013, 40(s1): s104001.
[6] Wang L, Wang J T, Yang J W, et al. 2.79 μm high peak power LGS electro-optically *Q*-switched Cr, Er∶YSGG laser[J]. Optics Letters, 2013, 38(12): 2150-2152.
[7] Fan M Q, Li T, Zhao S Z, et al. Watt-level passively *Q*-switched Er∶Lu_2O_3 laser at 2.84 μm using MoS_2[J]. Optics Letters, 2016, 41(3): 540-543.
[8] Fan M Q, Li T, Zhao S Z, et al. Multilayer black phosphorus as saturable absorber for an Er∶Lu_2O_3 laser at ~3 μm[J]. Photonics Research, 2016, 4(5): 181-186.
[9] Nie H K, Zhang P X, Zhang B T, et al. Watt-level continuous-wave and black phosphorus passive *Q*-switching operation of Ho_3, Pr_3∶$LiLuF_4$ bulk laser at 2.95 μm[J]. IEEE Journal of Selected Topics in Quantum Electronics, 2018, 24(5): 1600205.
[10] Wei C, Zhu X S, Wang F, et al. Graphene *Q*-switched 2.78 μm Er^{3+}-doped fluoride fiber laser[J]. Optics Letters, 2013, 38(17): 3233-3236.
[11] Könz F, Frenz M, Romano V, et al. Active and passive *Q*-switching of a 2.79 μm Er∶Cr∶YSGG laser[J]. Optics Communications, 1993, 103(5/6): 398-404.
[12] Vodopyanov K L, Shori R, Stafsudd O M. Generation of *Q*-switched Er∶YAG laser pulses using evanescent wave absorption in ethanol[J]. Applied Physics Letters, 1998, 72(18): 2211-2213.
[13] Kisel V E, Shcherbitskii V G, Kuleshov N V, et al. Saturable absorbers for passive *Q*-switching of erbium lasers emitting in the region of 3 μm[J]. Journal of Applied Spectroscopy, 2005, 72(6): 818-823.
[14] Inochkin M V, Korostelin Y V, Landman A I, et al. A compact Er∶YLF laser with a passive Fe^{2+}∶ZnSe shutter[J]. Journal of Optical Technology, 2012, 79(6): 337-339.
[15] Velikanov S D, Gavrishchuk E M, Zakharov N G, et al. Efficient operation of a room-temperature Fe^{2+}∶ZnSe laser pumped by a passively *Q*-switched Er∶YAG laser[J]. Quantum Electronics, 2017, 47(9): 831-834.
[16] Degnan J J. Theory of the optimally coupled *Q*-switched laser[J]. IEEE Journal of Quantum Electronics, 1989, 25(2): 214-220.
[17] Dong J. Numerical modeling of CW-pumped repetitively passively *Q*-switched Yb∶YAG lasers with Cr∶YAG as saturable absorber[J]. Optics Communications, 2003, 226(1/2/3/4/5/6): 337-344.

Theoretical Analysis and Experimental Study of Pulse Characteristics of Fe^{2+}∶ZnSe Passively *Q*-switched 2.794 μm Laser with High Repetition Rate

Xiong Zhengdong[1,2], Jiang Lingling[1,2], Cheng Tingqing[1], Jiang Haihe[1,2*]

[1]*Institute of Health and Medical Technology, Hefei Institutes of Physical Science, Chinese Academy of Sciences, Hefei* 230031, *Anhui, China*;

[2]*University of Science and Technology of China, Hefei* 230031, *Anhui, China*

Abstract

Objected Lasers with high repetition rate and nanosecond pulse width around 3 μm waveband are required to improve the conversion rate of optical parameters and reduce the thermal effect when they are used in mid-infrared parametric pumping and hard tooth tissue ablation. The *Q*-switched technology is widely used to generate lasers with high peak power and narrow pulse width. Currently, the high-peak-power laser output at 3 μm waveband has been obtained using electro-optic *Q*-switched laser technology. However, because of the thermal depolarization effect of polarized laser under high-power pump, the repetition frequency of electro-optic *Q*-switched technology cannot be increased. The high repetition frequency can be achieved using acousto-optic *Q*-switched technology, but the large laser pulse energy cannot be realized owing to the limitation of the diffraction efficiency of the acousto-optic device. Mechanical *Q*-switched technology cannot produce stable laser pulses because it is difficult to accurately control the motor during high-speed operations. Theoretically, a passively *Q*-switched laser can achieve nanosecond laser pulses with high repetition frequency and high peak power as long as the damage threshold of the optical components is sufficiently large. Moreover, as a passively *Q*-switched laser has a compact cavity structure, its use is advantageous in laser applications.

Many materials have been proved to be suitable for passively *Q*-switched lasers in the 3 μm waveband, and only a few relatively stable materials such as Fe^{2+}∶ZnSe crystals can achieve a large energy output. However, as the Fe^{2+}∶ZnSe crystal has a low damage threshold (1.5–2.0 J/cm^2@100 ns) in the 3 μm waveband, it can easily be damaged when operating at high peak power and high repetition frequency. Hence, to reduce the risk of damage during normal operation, it is necessary to analyze the pulse characteristics of Fe^{2+}∶ZnSe crystals in passive *Q*-switched lasers to reduce the possibility of damage to the saturable absorber and realize laser operation at a high peak power and high repetition rate.

Methods Using output mirrors with different reflectivities, the values of the output pulse width of a Fe^{2+}∶ZnSe saturable absorber are theoretically calculated (Fig. 1 and Table 1). The values provide theoretical guidance for the design of passively *Q*-switched lasers. The pulse widths under two initial transmittances of the Fe^{2+}∶ZnSe crystal (91.9% and 93.6%) and two reflectivities of the output mirror (30% and 40%) are measured using Er, Cr∶YSGG laser crystal rods with two sizes (Φ3 mm×100 mm and Φ4 mm×100 mm) pumped by a xenon lamp (Fig. 2). The theoretical calculation results are verified through relevant experiments.

Based on the measurement results, a high-repetition-rate Fe^{2+}∶ZnSe crystal passively *Q*-switched laser system with a concave-

convex resonator structure is developed to compensate for the thermal focal length. The Er, Cr∶YSGG crystal has dimensions of Φ3 mm×100 mm. Concave mirror M_1 is used as the all-reflection mirror (R_1=200 mm), M_2 is used as the output mirror (R_2=−216 mm), and the reflectivity of the convex surface is 70% at 2.79 μm.

Results and Discussions The results in Table 1 and Fig. 3 show that the pulse width of the output lasers with different initial transmittances narrows with an increase in the reflectivity of the output mirror. A passively *Q*-switched laser output with large energy and narrow pulse width can be obtained more easily when the initial transmittances of the saturable absorber are lower. The experimental results verify the accuracy of the calculation. Moreover, the pulse width of the laser output has little relation with the size of the laser crystal rod, and the pulse widths obtained with the crystal rods with two different sizes are similar. From the beam diameter in the cavity, it is observed that a larger crystal rod diameter changes the mode volume in the cavity and increases the output laser energy; however, the laser energy density in the cavity does not increase because the bleaching process of the saturable absorber is not affected by the increase in the beam diameter.

By optimizing the internal component layout of the 60 Hz Er, Cr∶YSGG passively *Q*-switched laser, the high repetition frequency and high peak power of the 2.794 μm passively *Q*-switched laser can be achieved. Figure 5 shows the experimental waveforms of the 60 Hz passively *Q*-switched laser with two Fe^{2+}∶ZnSe crystals. The single pulse energy of the lasers is 4.7 mJ and 7.0 mJ, with pulse widths of 97.0 ns [Fig. 5 (a)] and 72.6 ns [Fig. 5 (c)], respectively.

Conclusions The results show that a saturable absorber with low initial transmittance can achieve a low pulse width, whereas a saturable absorber with high initial transmittance can compress the pulse width by enhancing the reflectivity of the output mirror. Based on these results, the xenon lamp pumping Er, Cr∶YSGG laser is optimized, and Fe^{2+}∶ZnSe passively *Q*-switched laser pulses with high repetition rate (60 Hz) and high peak power (7.0 mJ) are realized.

Key words lasers; solid-state lasers; Er, Cr∶YSGG laser; passive *Q*-switching; Fe^{2+}∶ZnSe